

On the *in situ* relaxation of interphase interfaces

J. G. ERLINGS, F. W. SCHAPINK

Laboratory of Metallurgy, Delft University of Technology, Rotterdamseweg 137, 2628 AL Delft, The Netherlands

A previously used method for the study of twist boundaries in Au bicrystals is extended to interfaces in Au/AuPd and Au/Pd bicrystals. Transmission electron microscopy and electron diffraction results of the relaxation of small-angle boundaries, boundaries close to the coherent twin orientation and epitaxial layers are reported and interpreted in terms of dislocation networks with Burgers vectors of the type $a/2 \langle \bar{1} 1 0 \rangle$ or $a/6 \langle 1 1 \bar{2} \rangle$.

1. Introduction

Phase-boundary structures observed by TEM in thinned bulk specimens have been studied by numerous authors [1-3]. In most of these investigations the phase boundary was inclined to the surface which limits the dimensions of the boundary plane. In addition, the relative orientation of the boundary-forming crystals and the orientation of the boundary plane cannot easily be adjusted thus limiting systematic research. Many systematic TEM studies [4-6] on well-defined grain boundaries in oriented bicrystals have been performed in the last decennium. An attempt to extrapolate these experiments to (100) Au/Ag twist phase boundaries has been made recently by Goodhew and Maheswaran [7].

In this paper a preliminary account of an investigation on (111) AuPd/Au twist-phase boundaries is reported. The results presented are an extension of previous experiments on (111) twist boundaries in Au [6, 8, 9] and (111) Au/Pd epitaxial bicrystals [10]. Particular attention is paid to the *in situ* relaxation of bicrystals containing small-angle boundaries and boundaries with a small deviation from the twin orientation.

2. Experimental details

(111) Au₇₅Pd₂₅/Au bicrystals containing unrelaxed twist-phase boundaries were prepared with twist angles ranging from 0° to 5° and 55° to 65°. The relative change in lattice parameter in the Au₇₅Pd₂₅-Au specimens (dilatation δ) is 0.010 to 0.015. In addition, a number of (111) Au/Pd

bicrystals with twist boundaries within the same twist angle region were prepared. Unrelaxed bicrystals were obtained by positioning gel-grown (111) Au single crystals [8] onto vapour-grown (111) Au₇₅Pd₂₅ or (111) Pd single-crystal films. The latter films were prepared by vacuum deposition on muscovite mica substrates (Pashley method) in an UHV evaporation apparatus described elsewhere [11]. Prior to deposition of these layers a 20 nm thick intermediate Ag layer was deposited on the mica. The alloy films were evaporated by simultaneous operation of two sources containing Au and Pd, respectively. All films were prepared at a pressure of 8×10^{-8} Pa. The evaporation rate was 0.2 nm sec⁻¹ and the substrate temperature was 525 K. From the AuPd or Pd/Ag/mica sandwich the Ag layer was dissolved in nitric acid whereafter the alloy film was picked up with a double-pitch Au grid (Au 75/300). The Pd film was subsequently heat treated for 5 min at 800 K in a HV system. During this heat treatment the Pd film started to break up locally, resulting in a perforated film.

Specimens were studied in a Philips EM400 electron microscope equipped with a STEM unit. Relaxation of the bicrystals was studied *in situ* using a heating stage. All micrographs and diffraction patterns were obtained at 120 kV.

3. Results and discussion

Thin (111) AuPd/Au bicrystal films containing unrelaxed (111) twist-phase boundaries form a very useful system to study systematically the

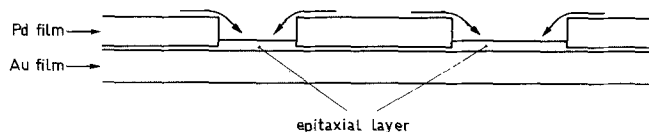


Figure 1 Schematic drawing of the Au/Pd bicrystal geometry during relaxation.

relaxation behaviour of twist boundaries between two crystals with the same symmetry and different lattice parameters. The major advantage of this system is the possibility of studying a series of phase boundaries with different jumps in lattice spacing across the boundary. This is due to the ability to vary continuously the lattice spacing of the AuPd fcc substitutional alloy with composition of the alloy. An important property of this metal couple is the adhesion between the AuPd and Au films. Although the superposition of the two crystals is performed in air, phase boundaries can still be formed by solid-phase bonding at slightly elevated temperatures in the electron microscope. This is in agreement with Tylecote [12] who suggested that heating of metals in vacuum removes the oxide layer and contamination, whereafter Au-metal solid-phase bonding may occur at slightly elevated temperatures. With this system the relaxation structure of a range of boundaries with different dilatation and twist components can be studied.

We will first discuss relaxation experiments on unrelaxed (111) Au/Pd twist boundaries. After heating for 2.5 h at temperatures in the range 473 to 668 K no relaxation effects could be observed in the boundary planes, probably due to oxidation of the Pd surface. This oxide layer prevented initial atomic contact between the two boundary-forming crystals. Subsequent heat treatment at a higher temperature (0.5 h at 734 K) resulted in surface diffusion of Pd into the holes in the Pd films, forming epitaxial layers on the Au crystals (see Fig. 1). In the interfaces of these *in situ* formed epitaxial bicrystals, misfit dislocation networks were observed. An example of such a network formed in a Au/Pd bicrystal containing a small-angle (2.4°) twist boundary is shown in Fig. 2a. The inset of this figure shows a schematic drawing of the part of the hexagonal network indicated by the arrow. A part of the image in Fig. 2a consists only of dislocation contrast, since by a proper adjustment of the objective aperture and employing a well-overfocused second condenser lens, only one ($\bar{2}20$) reflection passed through the objective aperture. The dislocation spacing in this network was between 6.6 and

7.3 nm and the average direction of the dislocation lines was parallel to the $\langle 1\bar{1}0 \rangle$ directions. From the corresponding diffraction pattern shown in Fig. 2b the dilatation misfit between the two layers was calculated to be 0.0225 to 0.0240. A number of weak reflections are present near the $\{\bar{2}20\}$ reflections which can be observed in an enlarged print of the area indicated in Fig. 2b (Fig. 2c). The geometry of the diffraction pattern in Fig. 2c is shown schematically in Fig. 2d. It should be noticed that from the diffraction pattern in Fig. 2b no information about the 2.4° twist boundary which surrounds the epitaxial layer can be obtained. Consequently, most of the diffraction information in Fig. 2b corresponds to the epitaxial area.

The epitaxial layer can grow on the (111) Au surface either in the single-crystal or in the twin orientation described by a rotation of 60° around the $[111]$ axis which is normal to the surface. These two boundary types should contain different interface structures [13]. In the single-crystal orientation, a dislocation network containing edge dislocations with $b = a/2 \langle \bar{1}10 \rangle$ is expected to accommodate the misfit while at the twin orientation a dislocation network containing edge dislocations with $b = a/6 \langle 11\bar{2} \rangle$ should exist. Such interfacial dislocation networks will give rise to extra reflections in electron diffraction patterns [14, 15]. When the incident beam is perpendicular to the interface these extra reflections can be distinguished from double diffraction when $b = a/2 \langle \bar{1}10 \rangle$ while reflections from the network with $b = a/6 \langle 11\bar{2} \rangle$ will coincide with double diffraction vectors [6]. In the case of Fig. 2, double diffraction is described by the difference vectors of the ($\bar{2}20$) reflections from both crystals. Applying this to Fig. 2d it is noticed that no extra reflections in addition to double diffraction can be observed indicating that the network consists of dislocations with $b = a/6 \langle 11\bar{2} \rangle$. In addition, the row of reflections left of the ($\bar{2}20$) reflections in Fig. 2d is neither observed in dislocation-free epitaxial crystals [10] nor in epitaxial crystals containing misfit dislocation networks with $b = a/2 \langle \bar{1}10 \rangle$ [16], which indicates that these reflections with the same geometry as double diffraction

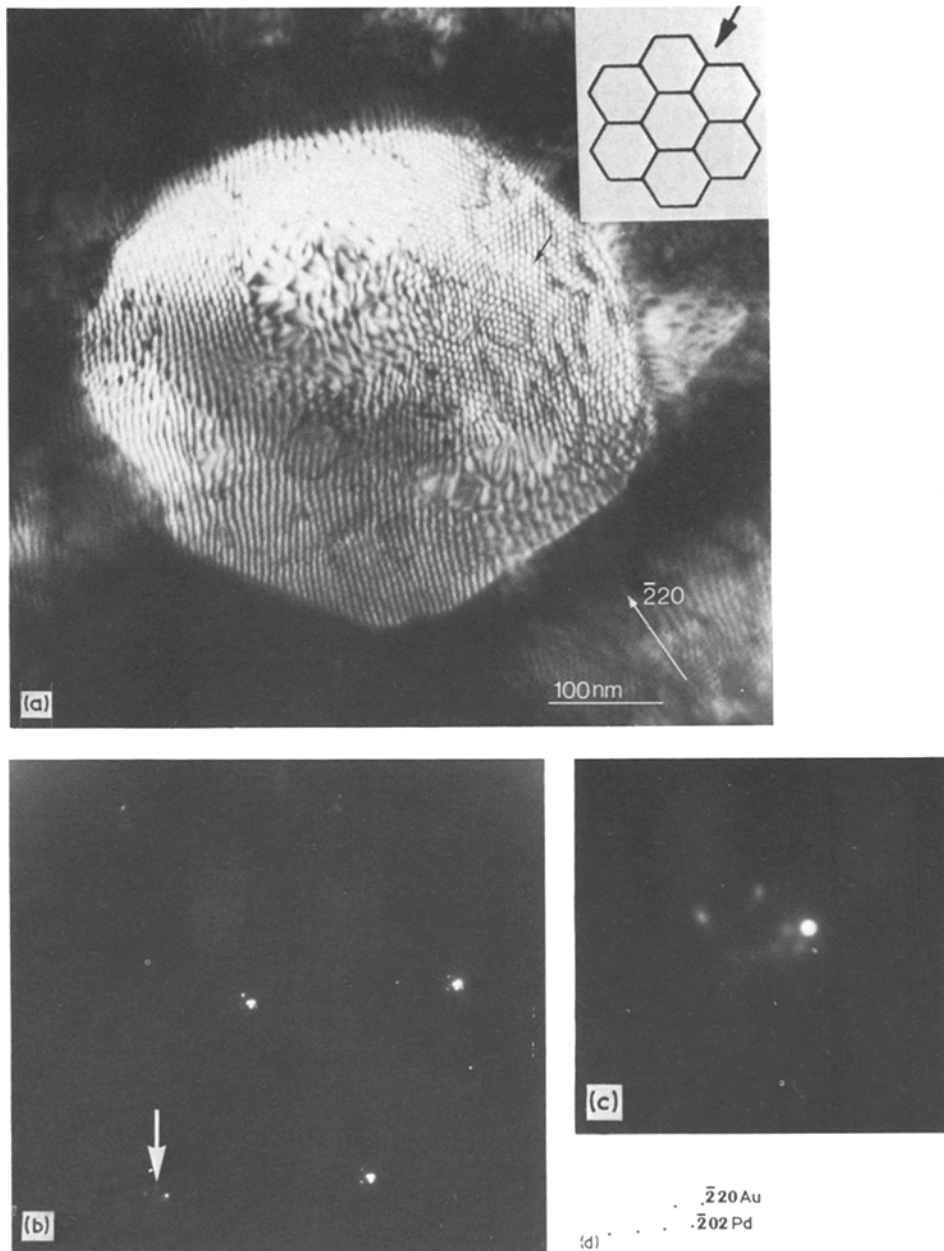


Figure 2 (a) A dislocation network in the interface of an *in situ* formed epitaxial Pd layer on an Au crystal (b) Selected-area diffraction pattern of the area in (a). (c) Enlarged photograph of the area indicated in (b). (d) Schematic drawing of (c).

originate from a dislocation network with $b = a/6 \langle 11\bar{2} \rangle$. If an edge dislocation network with $b = a/6 \langle 11\bar{2} \rangle$ accommodates the misfit of 0.0225 to 0.0240, the dislocation spacing is 6.9 to 7.4 nm with the dislocation line directions parallel to the $\langle \bar{1}10 \rangle$ directions. This is in agreement with the observed network in Fig. 2a, which shows that the epitaxial layer is in the twin orientation.

The observed misfit of 0.0225 to 0.0240 is less than the theoretical misfit of 0.046 between pure Au and pure Pd. The difference is probably due to alloying of the bicrystals and a strain in the Pd layer which was also observed by other authors [17, 18].

Next the results of *in situ* relaxation of Au/AuPd low-angle twist boundaries ($\delta = 0.010$ to 0.015)

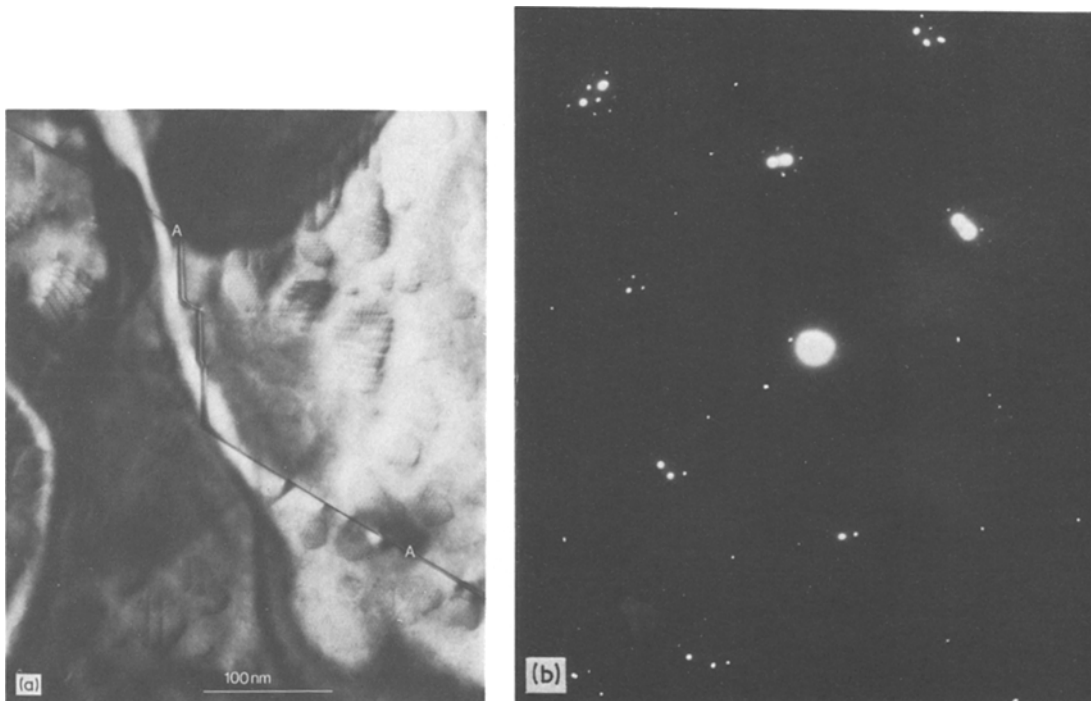


Figure 3 (a) Dislocation networks in a partly relaxed Au/AuPd small-angle twist boundary ($\theta = 3.6^\circ$, $\delta = 0.005$). (b) Selected-area diffraction pattern of the area indicated in (a).

will be discussed. During heat treatment at 800 K the formation of dislocation networks can be observed locally (Fig. 3a). In the dislocation networks in Fig. 3a lines are visible which are lattice dislocations interacting with the network. The straight lines in Fig. 3a result from the intersection of the surface with coherent twin boundaries which are formed during deposition of the alloy on the Ag/mica substrate [19]. The boundary planes are $\{11\bar{2}\}$ planes perpendicular to the surface, which intersect the surface along $\langle\bar{1}10\rangle$ directions. The evaporated layer can grow either in the matrix orientation (M) or in the twin orientation (T), as noted earlier in this section. The presence of these two orientations has been con-

firmed with dark-field microscopy using $(\bar{1}11)$ type reflections. As a result of twinning in the AuPd layer small-angle boundaries as well as boundaries with small deviations from the coherent twin orientation are present in the Au/AuPd interface (Fig. 4). The configurations of these boundaries in the relaxed state can be described analogous to the relaxation of similar twist grain boundaries in Au [6]. The misfit in the low-angle boundary will be localized in dislocation networks with $b = a/2 \langle\bar{1}10\rangle$ while in the near-coherent twin boundary a dislocation network with $b = a/6 \langle 11\bar{2}\rangle$ will accommodate the misfit. The dislocations in these boundaries are of mixed screw and edge type due to the combination of a rotation and dilatation at the boundary.

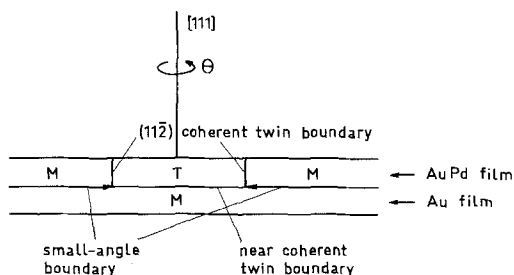


Figure 4 Schematic drawing showing the geometry of the unrelaxed Au/AuPd bicrystals.

The dislocation line directions can easily be calculated from Bollmann's O-lattice [20] by identifying the dislocation lines with the Wigner-Seitz cell walls of the O-lattice. The angle (ξ) between the dislocation line directions and $\langle\bar{1}10\rangle$ direction of the gold crystal is given by

$$\cot \xi = \frac{\delta' \sin \theta}{1 - \delta' \cos \theta} \quad (1)$$

where $\delta' = 1 - \delta$. The dependence of the rotation ξ of the dislocation line direction on δ and θ is

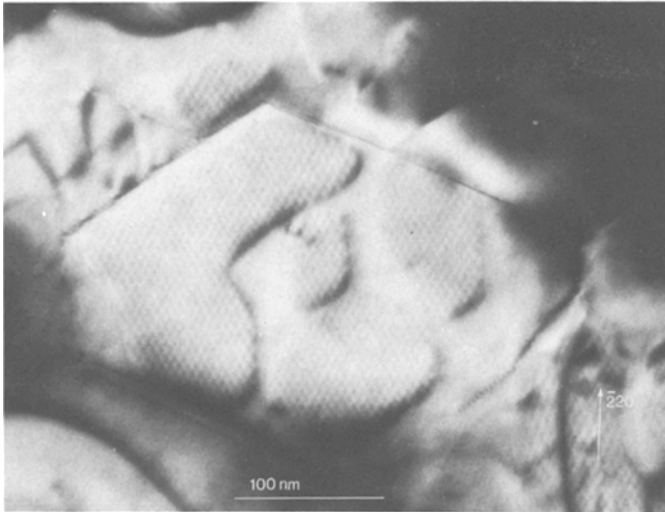


Figure 5 Dislocation network in a relaxed part of a small-angle twist-phase boundary ($\theta = 3^\circ$, $\delta = 0.005$).

similar to the behaviour of Moiré patterns as discussed by Bassett *et al.* [21].

A dislocation network in a partly relaxed small-angle boundary ($\delta = 0.005$ and $\theta = 3^\circ$) is shown in Fig. 5. Assuming $b = a/2 \langle \bar{1} 1 0 \rangle$, the calculated dislocation spacing is 5.5 nm which is in reasonable agreement with the measured spacing of 6.0 nm. The dislocation line directions are nearly parallel to the $\langle \bar{1} 1 0 \rangle$ directions which agrees with a calculated value for ξ of 7° .

From Equation 1 it is found that the angle ξ increases at higher dilatations or small twist angles; for example at $\delta = 0.02$ and $\theta = 3^\circ$ this angle is

22.6° and at $\delta = 0.005$ and $\theta = 1^\circ$ this angle is 16.5° . For this reason we suggest that especially for boundaries with small misorientations important information can be obtained from dislocation line directions. Extra reflections due to diffraction from dislocation networks in low-angle boundaries emerged during heat treatment of unrelaxed bicrystals. Fig. 6a is a selected-area diffraction pattern of a boundary with $\theta = 4.3^\circ$ and $\delta = 0.014$. The reflections indicated in the inset were not present initially but emerged during heat treatment. In Fig. 6b a Riecke micro-diffraction pattern taken from one side of the twin boundary A–A

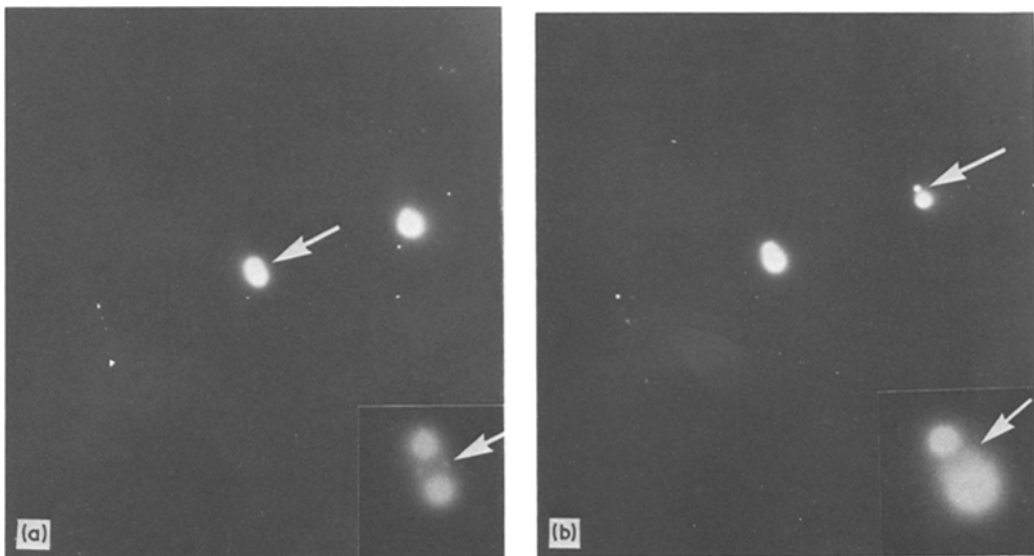


Figure 6 (a) Selected-area diffraction pattern of a boundary ($\theta = 4.3^\circ$, $\delta = 0.014$) containing dislocation networks with $b = a/2 \langle \bar{1} 1 0 \rangle$. Extra reflections due to these networks are indicated in the inset. (b) Riecke micro-diffraction pattern from a relaxed area in Fig. 3a.

in Fig. 3a shows extra reflections at positions indicated on the inset. Similar patterns from the other side of the line A—A showed no extra reflections, although networks can be observed at both sides. This agrees with expectations based on Fig. 4, which shows that twin boundaries in the AuPd film separate regions with small-angle boundaries and boundaries with a small deviation from the coherent twin orientation.

4. Conclusions

(1) With the experimental technique described, a systematic study of the *in situ* relaxation of boundaries between both rotated and dilatated crystals is possible.

(2) An example is discussed of an epitaxial Pd layer growing *in situ* on a (111) Au substrate where the misfit in the interface is located in dislocation networks with $b = a/6 \langle 11\bar{2} \rangle$.

(3) *In situ* relaxation of low-angle twist-phase boundaries and phase boundaries with a small deviation from the twin orientation can be described in a way analogous to the relaxation of similar grain boundaries.

References

1. H. I. AARONSON, *J. Microsc.* **102** (1974) 275.
2. H. I. AARONSON, H. B. AARON and K. R. KINSMAN, *Metallogr.* **4** (1971) 1.

3. G. C. WEATHERLY, *Met. Sci. J.* **2** (1968) 25.
4. R. W. BALLUFFI, Y. KOMEN and T. SCHOBER, *Surf. Sci.* **31** (1972) 68.
5. W. R. WAGNER and R. W. BALLUFFI, *Phil. Mag.* **30** (1974) 673.
6. J. G. ERLINGS and F. W. SCHAPINK, *Phys. Stat. Sol. (a)* **52** (1979) 529.
7. P. J. GOODHEW and P. MAHESWARAN, Proceedings of Micro 78, *Roy. Microsc. Soc.* **13** (4) (1978) 54.
8. J. G. ERLINGS and F. W. SCHAPINK, *Scripta Met.* **11** (1977) 427.
9. *Idem*, *Phys. Stat. Sol. (a)* **46** (1978) 653.
10. *Idem*, *Thin Solid Films* **61** (1979) 33.
11. J. G. ERLINGS and H. WEERHEIJM, in preparation.
12. R. F. TYLECOTE, *Gold Bull.* **11** (1978) 74.
13. D. H. WARRINGTON and H. GRIMMER, *Phil. Mag.* **30** (1974) 461.
14. J. SPYRIDELIS, P. DELAVIGNETTE and S. AMELINCKX, *Mater. Res. Bull.* **2** (1967) 615.
15. C. J. FORWOOD and L. M. CLAREBROUGH, *Phil. Mag.* **36** (1977) 1131.
16. D. CHERNS, *Thin Solid Films* **48** (1978) 385.
17. J. W. MATTHEWS, *Phil. Mag.* **13** (1966) 1207.
18. A. M. BEERS and E. J. MITTEMEIJER, *Thin Solid Films* **48** (1978) 367.
19. J. W. MATTHEWS, *Phil. Mag.* **7** (1962) 915.
20. W. BOLLMANN, "Crystal Defects and Crystalline Interfaces" (Springer Verlag, Berlin, 1970).
21. G. A. BASSETT, J. W. MENTEN and D. W. PASHLEY, *Proc. Roy. Soc. A* **246** (1958) 345.

Received 31 May and accepted 16 July 1979.